RSC Advances

PAPER

View Article Online
View Journal | View Issue

Cite this: *RSC Adv.*, 2019, **9**, 7587

Design, synthesis and properties investigation of N^{α}-acylation lysine based derivatives†

Ting-Ting Shi,[ab] Zheng Fang,[a] Wen-Bo Zeng,[a] Zhao Yang,[c] Wei He[a] and Kai Guo *[ad]

Received 10th January 2019
Accepted 27th February 2019

DOI: 10.1039/c9ra00213h

rsc.li/rsc-advances

Amino acid-based compounds have attracted attention as environmentally friendly bio-based materials. Our group has recently developed a novel family of N^{α}-acylation lysine based derivatives. We introduced long chain acyl groups at the N^{α} position selectively by a new synthetic route that avoided the process of amino protection and deprotection. Sodium N^{α}-octanamide lysine (C8), sodium N^{α}-capramide lysine (C10) and sodium N^{α}-lauramide lysine (C12) can self-assemble into vesicles spontaneously. As a result, not only do they have potential in drug delivery system but also they may be used as bio-based surfactants applied in cosmetics and other industries.

Introduction

The consumption of surfactants is quite large since surfactants are widely used in households and industries. Traditional surfactants are derived from petrochemical compounds which are non-renewable resources, such as crude oil and coal.[1] Besides, chemically-synthesized surfactants are not biodegradable and are toxic to the soil and organisms.[2] Compared with traditional surfactants, bio-based surfactants perform sustainably and are friendly to the environment since they have a natural origin.[3] Recently, amino acid-based surfactants have been shown to have outstanding performance due to their enhanced biodegradability,[4] biocompatibility and low ecotoxicity,[5] as well as the excellent properties derived from their peculiar structures.[6] By introducing hydrophobic groups in the carboxylic or amino groups of amino acids it is possible to synthesize anionic, cationic, and amphoteric surfactants.[7] The hydrophobic tails can be synthons with different structures, lengths, and numbers.[6,8]

Considering the application of surfactants associated with the surface activities and the self-assembly properties, several studies paid attention to the aqueous solution aggregation properties of lysine-based derivatives. Brito *et al.*[9] studied the self-assembly of sodium $N^{\alpha}N^{\varepsilon}$-lysine derived surfactants synthesized with the use of 2-(1*H*-benzotriazole-1-yl)-1,1,3,3-tetramethyl uranium tetrafluoroborate (TBTU) as condensation agent. These surfactants show a rich phase behaviour ranging from tubules to catanionic vesicles, moreover, they present a reverse hexagonal to smectic phases as liquid crystalline behaviour. Lourdes *et al.*[10] synthesized long chain N^{ε}-acyl lysine methyl ester salts using the N^{α}-Cbz-lysine. The N^{ε}-lysine methyl ester salts have low CMC values and can be good candidates in biomedical applications. In the last decades, studies on the synthesis and cytotoxicity behaviour[11] as well as concentration studies[9c] of $N^{\alpha}N^{\varepsilon}$- or N^{ε}-lysine based amphiphiles have also been reported.

On the basis of current surfactants work, we can find almost all the reports concerning lysine were about $N^{\alpha}N^{\varepsilon}$- or N^{ε}-lysine based derivatives. Despite they have good surface activities and a lot of potential application, the synthetic process of them are a little complicated which causes little prospect of industrialization. However, there are rare researches about the surface activities or self-assembly properties of N^{α}-lysine based derivatives, because it is difficult to get N^{α}-lysine based derivatives from lysine directly. On account of the electronic effect and solvation effect, N^{α}-lysine has higher activity than N^{ε}-lysine. Therefore, we decorated lysine at N^{α} position with acyl group which may have a good surface activities as other *N*-acylamino acid-based derivatives (Fig. 1).

In this work, we obtained several sodium N^{α}-lysine based derivatives with varying even chain length and investigated their self-assembling properties in aqueous medium. The main purpose of our studies was to explain the influence to surface activities and crystal behaviour of these compounds by different structural parameters.

Results and discussion

Synthesis of N^{α}-lysine based derivatives

N^{α}-Lysine based derivatives were synthesized from lysine by three steps. First, heating the L-lysine in *n*-hexyl alcohol to obtained α-amino-ε-caprolactam (ACL). Then, acyl chloride reacted with ACL to get the α-amide-ε-caprolactam. More details on

[a]College of Biotechnology and Pharmaceutical Engineering, Nanjing Tech University, Nanjing 211816, P. R. China. E-mail: guokai@nitech.edu.cn
[b]Department of Chemistry, Bengbu Medical College, 233030, P. R. China
[c]School of Engineering, China Pharmaceutical University, No. 639 Longmian Avenue, Nanjing 211198, China
[d]State Key Laboratory of Materials-Oriented Chemical Engineering, Nanjing Tech University, Nanjing 211816, P. R. China

† Electronic supplementary information (ESI) available. See DOI: 10.1039/c9ra00213h

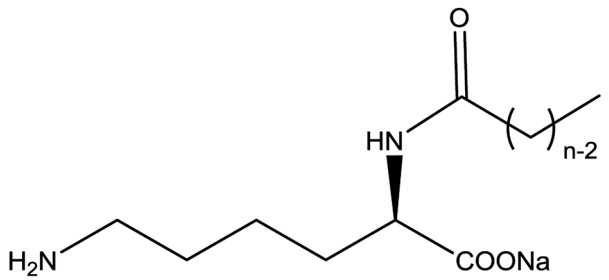

Fig. 1 Chemical structure of the N^{α}-lysine based derivatives; $n = 6$ (C6), $n = 8$ (C8), $n = 10$ (C10), $n = 12$ (C12), $n = 14$ (C14), $n = 16$ (C16), $n = 18$ (C18).

the synthesis about the intermediates are reported in the literature.[12] Finally, the hydrolysis happened in aqueous solution under alkaline conditions. Butanol was used to increase the solubility when the hydrophobic carbon number is larger than 12. According to the literature,[13] N^{α}-lauroyl lysine was obtained by preparing Cu ligand, making Cu complex of α-NH_2 and COOH group, protection of ε-NH_2, acylation of α-NH_2, deprotection of ε-NH_2. Compared with the literature, our route (Scheme 1) has less steps and higher yield.

Surface tension study

The surface tension method is a useful and accurate method for determining the surface properties. Similar to 12Lys12 (ref. 9*a* and 10*a*), measurements were done at 25 °C for C8 and C10, but 45 °C for C12 because of the low solubility at room temperature over 24 h in the full concentration range explored. Since the hydrophobic properties are hardly observed when the length of the hydrocarbon chain is too short (below 8 carbon),[14] we didn't report the relevant data about C6.

Fig. 2 clearly shows that the aqueous solutions of N^{α}-lysine based derivatives follow a conventional micelle-forming behaviour like other lysine based surfactants.[9a,10a] The critical micelle concentration (CMC) and surface tension value at the CMC (γ_{CMC}) is obtained at the break point in the surface tension *versus* log(concentrations) curve. Other surface-active parameters[15] such as the efficiency of adsorption pC_{20} (negative logarithm of surfactant concentration required to reduce the surface tension of water by 20 units) and the effectiveness of surface tension reduction Π_{CMC} (the difference of the surface

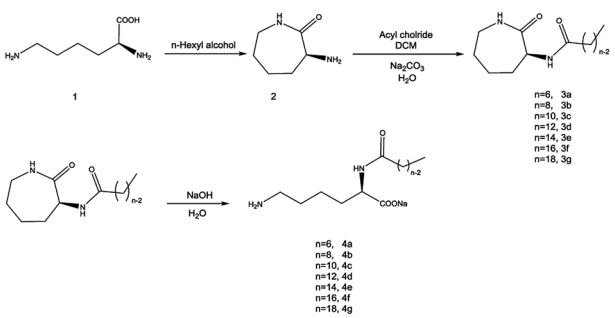

Scheme 1 Synthetic procedure used to obtain N^{α}-acylation lysine based derivatives ($n = 6$, 8, 10, 12, 14, 16, 18).

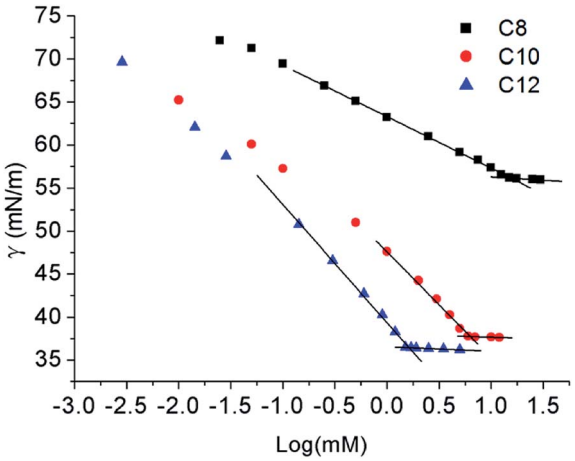

Fig. 2 Surface tension *versus* log (concentration) graphs for N^{α}-lysine based derivatives.

tension between pure water and solution at CMC) are determined from the surface tension plot in Table 1.

As expected, with increasing concentrations, surface tension values decrease until a plateau attributed to the happening of self-assemble. The γ_{CMC} decreases with increasing hydrophobic carbon number from 8 to 12. γ_{CMC} value of C8 was much higher than C10 and C12 which indicated that shorter hydrophobic chain of N^{α}-lysine based derivatives had a weaker ability to reduce surface tension. For C12, the surface tension values agree with the earlier reports of Rosen *et al.*,[16] γ_{CMC} changes between 31.5 and 38.0 mN m^{-1} for *N*-trimethylated cationic surfactants with 12–16 carbon atoms. Π_{CMC} values of C10 and C12 also demonstrate that they are more effective than C8 in reducing surface tension.

Regarding the CMC values obtained at the slope discontinuity in the surface tension *vs.* log(*C*) plots also decreased with increasing length of their hydrophobic chain. The CMC value of C8 is too large to calculate some surface active parameters, while the CMC values of C10 and C12 were similar low corresponding to other lysine based surfactants.[9a,9c,10a] We did not present the CMC value of C14 and above in this paper since they cannot be solved well even the temperature went up to 60 °C. No other break point was observed of the surface tension plot which points out the presence of none surface-active impurity.[9a]

A_{min} decreased with the increase of the hydrocarbon chain length which suggested the N^{α}-lysine based derivatives with longer hydrocarbon chain have higher packing density. Although the size of hydrophilic head group is a dominant factor to determine the values of Γ_{max} and A_{min},[16] longer hydrocarbon chain makes values of Γ_{max}[15b,17] higher since amphipathic molecules pack more closely and hydrophobic interactions are enhanced. Moreover, the compound with stronger hydrophobicity has a lower A_{min} value which can promote adsorb at the air–water interface. Besides, dialkyldimethylammonium surfactants[9b,18] have the similar behaviour. The intermolecular hydrogen bonding caused by N–H and C=O groups can also facilitate the packing of the molecules at the interface to enhance the surface adsorption.[9b,19] It is observed that pC_{20} value increased slightly from C10 to C12. The

Table 1 Surface properties of N^{α}-lysine based derivatives in aqueous solutions

Surfactant	CMC mM	γ_{CMC} mN m^{-1}	Π_{CMC} mN m^{-1}	C_{20}	pC_{20}	CMC/C_{20}	Γ_{max} μmol m^{-2}	A_{min} nm^2
C8	15.07	56.288	16.35	—	—	—	1.05	1.58
C10	7.64	37.724	34.91	0.29	3.54	14.11	1.84	0.90
C12	1.79	36.417	36.22	0.09	4.05	21.14	2.14	0.78

high pC_{20} value indicates that the effectiveness of these compounds in reducing the surface tension at the air/water interface is powerful which is similar to Gemini surfactants.[20] Larger CMC/C_{20} ratio has greater tendency to adsorb at the interface than to form micelles in solution which can be seen from Table 1 that C12 was easier to adsorb at the air/water interface than self-assemble in solution than C10. The result was in accordance with the conclusion of pC_{20}.

Aggregation behavior of derivatives solution

The aqueous solutions for C8, C10 and C12 with the concentration of 3 times and 5 times CMC were prepared, respectively. High purity Millipore water was used. C8 and C10 solutions were heated at 25 °C, and C12 was heated at 45 °C until translucent solutions appeared. The actual morphology of N^{α}-lysine based derivative aggregates in aqueous medium was studied using transmission electron microscopy (TEM) and dynamic light scattering (DLS). The TEM images (Fig. 3(a)–(c)) clearly exhibit the presence of almost uniformly distributed spherical vesicles. The inner diameters range of C8, C10 and C12 approximately from 30 to 80 nm. DLS measurement was carried out to provide exact information about the size of aggregates formed in aqueous solution. The results (Fig. 4) get from DLS show that diameters of the vesicles for the three compounds indeed range between 30 nm and 150 nm. Average diameters were 105.8 nm for C8, 82.7 nm for C10 and 74.5 nm for C12. With increasing the hydrocarbon chain length, the average diameters decreased. The result that the length of hydrocarbon chain influences the shape of aggregate is similar to the surfactants behavior of 2CAmGlu and CDLPB.[15a,21] We noticed the mean hydrodynamic diameters of the vesicles obtained from DLS were larger than TEM measurement. This might be due to the heating drying of the sample in TEM method, which is consistent with the study of T. Patra.[22]

The supramolecular arrangement of the vesicles can be explained by the existence of hydrophilic/lipophilic, electrostatic, van der Waals and H-bonding interactions between the surfactant molecules. To examine whether exist any hydrogen-bonding interactions in the self-assembly vesicles of C12, a FT-IR spectrum (Fig. 5) was measured in D_2O solvent. A broad peak at 3405 cm^{-1} can be seen, which is corresponding to the O–H stretching. This suggests that hydrogen-bonding interactions play a role in the self-organization of C12 molecules. The similar broad hydrogen bond peak at 3404 cm^{-1} presented by –OH group was also reported by Arjun Ghoshearlier.[23]

N^{α}-Lysine based molecules spontaneously form vesicles in solution at extremely low concentrations without external forces such as a supersonic wave. Not only they have potentials as drug delivery and model systems of bio-membranes[24] but also they are hopefully widen the application of polyoxometalate-based materials and device in probe dopamine against various biological molecules.[25]

Aggregation properties at high concentrations

Some interesting properties of N^{α}-lysine based derivatives were found when their length of hydrophobic carbon chain and concentrations changed.

The X-ray diffraction (XRD) patterns for C8, C10 and C12 are shown in support information. All three compounds have obvious peaks that mean these compounds are crystal form.

For C12, dispersed solid will be observed when the concentration was increased to 0.1 wt% at 25 °C in water. After heated to 45 °C, isotropic solution is obtained. Cooling the isotropic solution to room temperature induces the self-assembly of C12

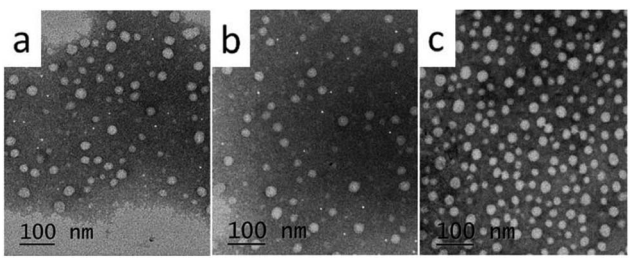

Fig. 3 TEM micrographs of N^{α}-lysine based derivatives solutions with 5 times the CMC: (a) C8, (b) C10, (c) C12.

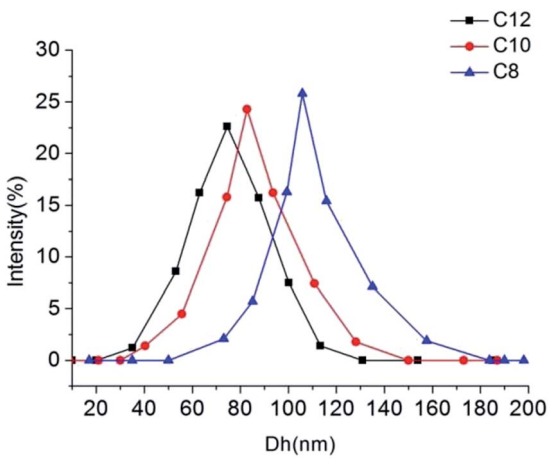

Fig. 4 DLS measurement of the size distributions of C8, C10 and C12 at 3 times the CMC.

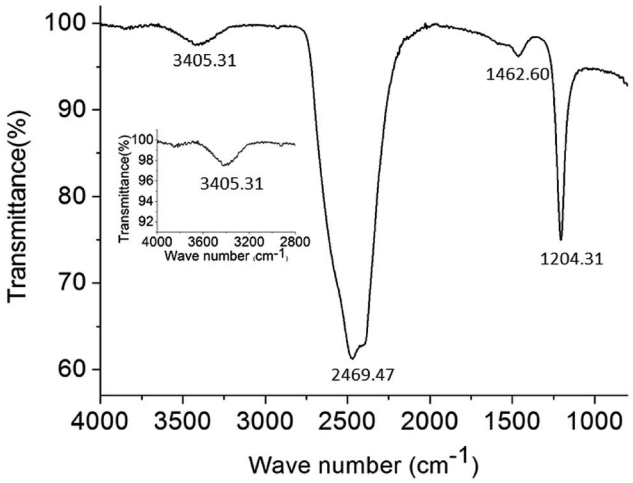

Fig. 5 FT-IR spectrum of 1 mM C12 in D_2O solvent; inset: H-bonded O–H region.

into entanglement. Above 0.8 wt% C12, a white gel-like sample formed efficiently traps all the solvent. As a function of concentration, the morphologies of the entanglement and gel were observed using optical microscopy. Fig. 6B1 shows that superstructures with some showing ramifications are observed. It precipitated into whiskers. The whiskers became shorter when the concentration increased.

It is well-known that the spontaneous curvature of a surfactant aggregate is related to the relative sizes of the hydrophilic head and hydrophobic tail of the surfactant molecule. Over the last decades many different structures lysine-based surfactants are reported to be formed supramolecular tubules or other three-dimensional structures.[9c,24b,26] Compared with these reports on gels of surfactants, sodium N^{α}-lauroyl lysine showed a new aggregation behavior.

C8 and C10 precipitated out from solution in the form of needle-like crystallites. More microscopic structures were observed by scanning electron microscopy (SEM) after the samples were simply dried in vacuum dryer. C10 was selected as the representative of needle crystal (Fig. 6A1). SEM showed that C10 aggregated to cuboid crystals (Fig. 6A2) while C12 tended to layered crystals, corresponding to a stack of lamellar plates (Fig. 6B2). The layered crystals revealed the formation of the whisker. The difference is probably due to steric hindrance of the alkyl chain, in addition, the different ordering or packing of the alkyl chains may also play an important role which is testified by FTIR below.

All the three compounds can gel without visible solvent separation with increasing the concentration. Amorphous appearance was observed by C12 under light microscopy. Parallel observations with optical polarizing microscopy provide complementary information concerning the identification of the amorphous phases. For the 25 wt% C12 (Fig. 6B3) a mosaic structure possibly hexagonal can be observed when the sample is visualized between crossed polarizers. For typical single-chained compounds, the phase sequence can change from micellar solution to hexagonal phase once the compound is fully hydrated.[9c] The gel phase behavior of C12 follows the common phase sequence. It may be the stronger hydrophobicity makes the molecules show a liquid crystal performance.

FTIR spectroscopic analysis was employed to provide an insight into the structure of the xerogels. The IR spectra (Fig. 7) of xerogels for the three compounds were nearly same, as two N–H stretchings, amide I, and amide II peaks appear at 3504, 3345, 1567, and 1536 cm^{-1}, respectively. Since there is no peak around 1710 cm^{-1} (the symmetric stretching vibration of –COOH), the molecules are presented as the deprotonated form $-COO^-$ peak appearing at 1619 cm^{-1}. The only difference observed is a peak at 1042 cm^{-1}, which is probably due to the different ordering or packing of the alkyl chains. A similar behavior is also seen for chiral urea gelators.[26]

Small angle X-ray scattering (SAXS) techniques are commonly used to determine the aggregate properties. After routine freeze-drying procedures, the assembly properties of dry N^{α}-lysine based surfactants were further analyzed using SAXS. According to Bragg equation:

$$2d \sin \theta = n\lambda \quad (1)$$

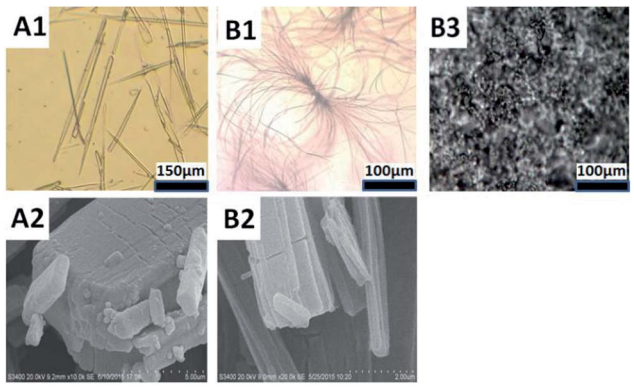

Fig. 6 Optical microscope images of supramolecular structures cooling from homogeneous aqueous solutions: (A1) 10 wt% C10; (B1) 1 wt% C12; (B3) 25 wt% C12, (B3) shows the optical texture when the sample is visualized between crossed polarizers. SEM images of supramolecular structures: (A2) C10; (B2) C12. A2 (bar = 5 nm) and B2 (bar = 2 nm).

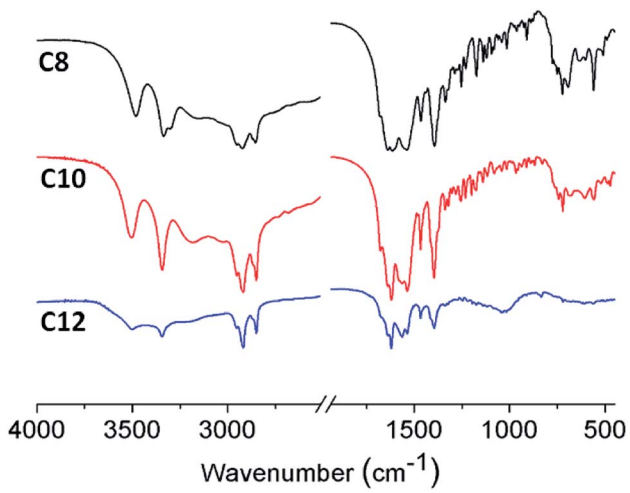

Fig. 7 FTIR spectras of C8, C10 and C12 in the dry state.

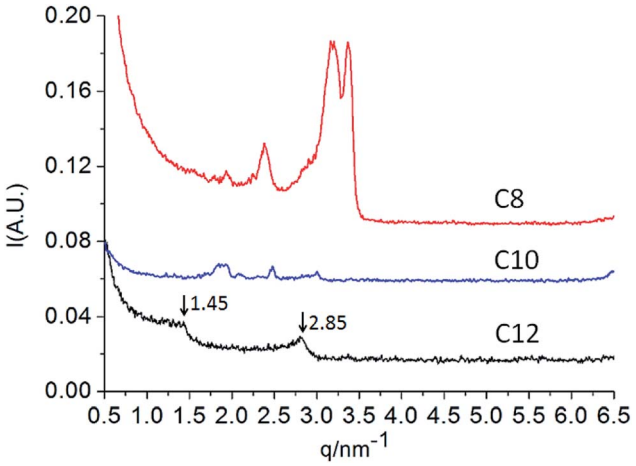

Fig. 8 SAXS curves for the three lysine based derivatives at 25 °C.

phase planes of liquid crystal with different structures have different proportional spacing. Bragg peak levels exhibit different proportion corresponding q factors in the SAXS curves.[27] The studies showed that only the C12 at dry state has distinct liquid crystalline behavior (Fig. 8). Two orders of peaks can be observed of C12, with q positions corresponding to 1 : 2 spacing, characteristic of lamellar structures (1 : 2 : 3).[10a,28]. The lamellar arrangements correspond to interdigitated hydrophobic chains, in which each hydrophobic chain interpenetrated with the hydrophobic tail of molecules corresponding to another leaflet. We can determine that the bilayer thickness corresponds to 2.14 nm and the bilayer spacing is 2.25 nm according to Bragg's law.[26,29] However, C12/water mixtures and dry state present a different liquid crystal behavior. The discrepancies may be present because of hydration. The possible multiple hydrogen bonds among hydrophilic groups of N^{α}-lauroyl lysine based compound are complicated. While the series of compounds deserve further investigation concerning the structuring of these mesophases may be obtained.

Conclusions

Seven N^{α}-lysine based derivatives from C6 to C18 were synthesized effectively by the new simple method. C8, C10 and C12 can self-assemble into vesicles spontaneously in aqueous solution which provided advantageous evidence of the potential application in drug and gene delivery. The lamellar phase of C12 was detected by PLM and SEM that may be applied in cosmetics as functional powder since van der Waal's force. Our research on N^{α}-lysine based compounds enriches the existing family of lysine-based derivatives. Considering the good performance of C10 and C12 in aggregation and surface activities, they deserve more attention and further research.

Experimental

General information

Lysine from biological source we used is donated by Hong Xu group, College of Biotechnology and Pharmaceutical Engineering, Nanjing Tech University. Other reagents were commercially available and used without further purification. Millipore water from a Milli-Q four-bowl system was used in all sample solutions.

The surface tension measurements were determined on a Kruss K100 Tensiometer (Kruss, Germany) using the ring method with an accuracy of 0.001 mN m^{-1}. The surface tension and subsequent experiments were all carried out at nature pH of the solution changing from 7 to 7.5. The maximum surface excess concentration, Γ_{max}, is calculated from the Gibbs adsorption eqn (2):

$$\Gamma_{max} = -\frac{1}{2.303nRT}\left(\frac{d\gamma}{d\log C}\right)_T \quad (2)$$

where R is the ideal gas constant (8.314J mol^{-1} K^{-1}), T is the absolute temperature, $d\gamma/d\log C$ is the slope of γ *vs.* $\log C$ profile at the point CMC and n is the number of free species at the interface ($n = 1$). The minimum surface area per molecule (A_{min}), at the air–water interface, is given by the eqn (3):

$$A_{min} = \frac{1}{N_A\Gamma_{max}} \times 10^{24} \quad (3)$$

where N_A is the Avogadro constant (6.022 × 10^{23} mol^{-1}).

TEM measurements were performed with a JEM-2100 transmission electron microscope (JEOL Ltd., Japan) at a working voltage of 200 kV. The samples were prepared using the negative staining method with 2% phosphotungstic acid solution. A droplet of the N^{α}-lysine based surfactant solution was placed on a copper grid by micropipette and allowed to equilibrate for 2 min. Excess liquid was carefully sucked out by touching one end of the grid with filter paper. The grid was dried under the lamp at 60 °C. Next, the phosphotungstic acid solution was added to the copper grid. The excess strain was absorbed after 3 min and then the samples were dried at 60 °C.

DLS measurements were carried out with a Zetasizer Nano ZS (Malvern Instrument Lab, Malvern, U.K.) light scattering spectrometer equipped with a He–Ne laser operated at 4 mW at $\lambda_0 = 633$ nm, a digital correlator, and a computer-controlled and stepping-motor-driven variable angle detection system. The measurement was done at 60 °C for the specimen.

An Olympus BX51 polarized light microscope was used. Images were acquired with an Olympus C5060 video camera and software CellA. After dispersing of the solid surfactant in high purity Milli-Q water and sonicated in a Bandelin Sonorex sonication bath, the sample was heated to 80 °C and then cooling down to obtain the sample.

SAXS measurements were performed at the BAMline at BESSY II (Berlin, Germany) with a Kratky-type instrument (SAXSess from Anton Paar, Austria). The SAXSess has a low sample-to-detector distance which is suitable for investigation of low scattering intensities. Routine freeze-drying procedures was taken to dry the samples. The samples were wrapped in aluminium foil and measured using a sample holder. The measured intensity was corrected by subtracting the intensity from aluminium foil. The SAXS scattering curves are shown as a function of the scattering vector modulus:

$$q = \frac{4\pi}{\lambda}\sin\theta/2 \quad (4)$$

where q is the scattering angle and λ is the wavelength of the radiation ($\lambda = 0.154$ nm). The q range obtained with our setup was from 0.5 to 6.5 nm^{-1}.

XRD data were recorded by an ARL X'TRA X-ray diffractometer at a scanning speed of 10° min^{-1}.

Scanning electron microscope imaging of the samples was done using a Hitachi S-3400N II scanning electron microscope. The samples were dried overnight in a vacuum before the observation.

FTIR spectra were obtained with a JASCO FT/IR-660 Plus. To obtain FTIR spectra, the gels were dried under vacuum. The dried samples and KBr were mixed and ground to form a fine powder under-lamp sample loading to avoid atmospheric moisture.

The elemental analyses measurements were performed with a Vario Micro cube (Elementar, Germany).

General procedure for the synthesis of N^{α}-acylation lysine based derivatives(4a–4f)

Water (100 mL), α-octanamide-ε-caprolactam (50 mmol, 12.7 g) and NaOH (100 mmol, 4.0 g) were added to the flask refluxing. After being stirred for 8 h, the solution was filtered while hot to remove insoluble impurities. The filtrate was cooled to room temperature then adjusted to neutral pH. Crude products were precipitated from water. After filtering, washing and drying, 13.7 g of sodium N^{α}-octanamide lysine was obtained.

Sodium N^{α}-hexanamide lysine (4a). Yield 85.8%; HRMS (ESI) for $C_{12}H_{24}N_2O_3$, m/z $[M + H]^+$: calcd 245.1820, found 245.1842; ^{1}H NMR (300 MHz, D_2O): δ 4.25 (dd, J = 8.3, 4.7 Hz, 1H, CHCOOH), 2.68 (t, J = 6.7 Hz, 2H, CH_2NH_2), 2.47–2.21 (m, 2H, CH_2CONH), 1.96–1.28 (m, 12H, CH_2), 0.97 (t, J = 6.5 Hz, 3H, CH_3). ^{13}C NMR (75 MHz, D_2O) δ 182.16–182.00 (m), 179.20 (s), 57.81 (s), 43.27 (s), 38.65 (s), 34.40 (d, J = 5.8 Hz), 33.33 (s), 27.84 (s), 25.42 (s), 24.44 (s), 16.05 (s). Elemental analysis for $C_{12}H_{23}N_2O_3Na$, calcd 266.16, C% calcd 54.12, found 54.17, H% calcd 8.71, found 8.74, N% calcd 10.52, found 10.48.

Sodium N^{α}-octanamide lysine (4b). Yield 93%; HRMS (ESI) for $C_{14}H_{28}N_2O_3$, m/z $[M + H]^+$: calcd 273.2133, found 273.2199; ^{1}H NMR (300 MHz, D_2O) δ 4.32 (s, 1H, CHCOOH), 3.13 (s, 2H, CH_2NH_2), 2.40 (s, 2H, CH_2CONH), 2.05–1.48 (m, 16H, CH_2), 0.99 (s, 3H, CH_3). ^{13}C NMR (75 MHz, D_2O) δ 180.80 (s), 178.17 (s), 57.20 (s), 42.20 (s), 38.79 (s), 34.37 (s), 34.03 (s), 31.68 (d, J = 15.6 Hz), 29.35 (s), 28.43 (s), 25.18 (s), 16.52 (s). Elemental analysis for $C_{14}H_{27}N_2O_3Na$, calcd 294.19, C% calcd 57.12, found 57.18, H% calcd 9.21, found 9.25, N% calcd 9.52, found 9.49.

Sodium N^{α}-capramide lysine (4c). Yield 90%; HRMS (ESI) for $C_{16}H_{32}N_2O_3$, m/z $[M + H]^+$: calcd 301.2446, found 301.2489; ^{1}H NMR (300 MHz, D_2O) δ 4.22 (s, 1H, CHCOOH), 3.05 (s, 2H, CH_2NH_2), 2.34 (s, 2H, CH_2CONH), 1.72–1.42 (m, 21H, CH_2), 0.95 (s, 3H, CH_3). ^{13}C NMR (75 MHz, D_2O) δ 181.36 (s), 177.44 (s), 57.62 (s), 42.02 (s), 38.88 (s), 34.62 (s), 34.30 (s), 32.63–31.87 (m), 29.33 (s), 28.49 (s), 25.16 (d, J = 19.6 Hz), 16.50 (s). Elemental analysis for $C_{16}H_{31}N_2O_3Na$, calcd 322.22, C% calcd 59.60, found 59.64, H% calcd 9.69, found 9.72, N% calcd 8.69, found 8.68.

Sodium N^{α}-lauramide lysine (4d). Yield 89%; HRMS (ESI) for $C_{18}H_{36}N_2O_3$, m/z $[M + H]^+$: calcd 329.2804, found 329.2812; ^{1}H NMR (MeOD, 300 MHz): δ 7.73 (s, 1H, CONH), 4.05–4.12 (m, 1H, CHCOOH), 2.98 (t, J = 6.0 Hz, 2H, CH_2NH_2), 2.51 (t, J = 1.5 Hz, 1H, COCHH), 2.17 (t, J = 7.2 Hz, 1H, COCHH), 1.23–2.12 (m, 24H, CH_2), 0.85 (t, J = 6.6 Hz, 3H, CH_3). ^{13}C NMR (75 MHz, MeOD) δ 179.36 (s), 175.21 (s), 53.28 (s), 41.43 (s), 33.48 (s), 32.23 (d, J = 1.5 Hz), 32.09 (s), 29.23 (dd, J = 18.5, 6.0 Hz), 25.99 (s), 23.25 (d, J = 16.0 Hz), 22.64 (s), 13.33 (s). Elemental analysis for $C_{18}H_{35}N_2O_3Na$, calcd 350.25, C% calcd 61.69, found 61.64, H% calcd 10.07, found 10.11, N% calcd 7.99, found 7.98.

Sodium N^{α}-myristamide lysine (4e). Yield 83%; HRMS (ESI) for $C_{20}H_{40}N_2O_3$, m/z $[M + H]^+$: calcd 357.3072, found 357.3113; ^{1}H NMR (300 MHz, MeOD) δ 4.31–4.18 (m, 1H, CHCOOH), 2.61 (t, J = 6.6 Hz, 2H, CH_2NH_2), 2.31–2.10 (m, 2H, $COCH_2$), 1.55–1.21 (m, 28H, CH_2), 0.93 (dd, J = 25.1, 7.0 Hz, 3H, CH_3). ^{13}C NMR (75 MHz, MeOD) δ 178.26 (s), 174.25 (s), 55.28 (s), 41.53 (s), 36.48 (s), 32.93 (d, J = 1.5 Hz), 32.01 (s), 29.53 (dd, J = 18.5, 6.0 Hz), 25.99 (s), 23.25 (d, J = 16.0 Hz), 22.65 (s), 13.37 (s). Elemental analysis for $C_{20}H_{39}N_2O_3Na$, calcd 378.29, C% calcd 63.46, found 63.50, H% calcd 10.39, found 10.42, N% calcd 7.40, found 7.38.

Sodium N^{α}-palmitamide lysine (4f). Yield 79%; HRMS (ESI) for $C_{22}H_{44}N_2O_3$, m/z $[M + H]^+$: calcd 385.3385, found 385.3425; ^{1}H NMR (400 MHz, D_2O) δ 4.07 (s, 1H, CHCOOH), 2.61 (s, 2H, CH_2NH_2), 2.18 (s, 2H, $COCH_2$), 1.67–1.46 (d, J = 36.4 Hz, 4H, CH_2), 1.20 (s, 28H, CH_2), 0.78 (s, 3H, CH_3). ^{13}C NMR (75 MHz, DMSO) δ 177.22 (s), 173.19 (s), 55.79 (s), 42.82 (s), 41.11 (d, J = 19.6 Hz), 40.68 (s), 40.40 (s), 40.12 (s), 37.43 (s), 34.52 (s), 34.18 (s), 32.85 (s), 30.78–29.87 (m), 26.95 (s), 24.07 (s), 23.59 (s), 15.01 (s). Elemental analysis for $C_{22}H_{43}N_2O_3Na$, calcd 406.32, C% calcd 64.99, found 65.03, H% calcd 10.66, found 10.69, N% calcd 6.89, found 6.87.

Sodium N^{α}-stearamide lysine (4g). Yield 75%; HRMS (ESI) for $C_{24}H_{48}N_2O_3$, m/z $[M + H]^+$: calcd 413.3698, found 413.3743; ^{1}H NMR (300 MHz, MeOD) δ 4.29–4.19 (m, 1H, CHCOOH), 2.61 (t, J = 6.9 Hz, 2H, CH_2NH_2), 2.30–2.15 (m, 2H, $COCH_2$), 1.74–1.54 (m, 6H, CH_2), 1.29 (s, 30H, CH_2), 0.89 (d, J = 6.8 Hz, 3H, CH_3). ^{13}C NMR (75 MHz, MeOD) δ 178.17 (s), 174.22 (s), 55.24 (s), 41.52 (s), 38.37 (s), 36.49 (s), 32.94 (s), 32.00 (s), 29.90–29.23 (m), 25.99 (s), 23.10 (s), 22.65 (s), 13.35 (s). Elemental analysis for $C_{24}H_{47}N_2O_3Na$, calcd 434.35, C% calcd 66.32, found 66.36, H% calcd 10.90, found 10.92, N% calcd 6.45, found 6.43.

Conflicts of interest

The authors declared that they have no conflicts of interest to this work.

Acknowledgements

We are grateful for the donation of lysine from Hong Xu Group, College of Biotechnology and Pharmaceutical Engineering, Nanjing Tech University. The research has been supported by the National Key Research and Development Program of China (2016YFB0301501), the National Natural Science Foundation of China (Grant No. 21776130), and the Jiangsu Synergetic

Innovation Center for Advanced Bio-Manufacture (XTD1821 and XTD1802).

Notes and references

1 S. Salati, G. Papa and F. Adani, *Biotechnol. Adv.*, 2011, **29**, 913.
2 (*a*) M. Lechuga, M. Fernández-Serrano, E. Jurado, J. Núñez-Olea and F. Ríos, *Ecotoxicol. Environ. Saf.*, 2016, **125**, 1; (*b*) M. J. Scott and M. N. Jones, *Biochim. Biophys. Acta*, 2000, **1508**, 235; (*c*) W. d. Wolf and T. Feijtel, *Chemosphere*, 1998, **36**, 1319.
3 R. Marchant and I. M. Banat, *Biotechnol. Lett.*, 2012, **34**, 1597.
4 (*a*) R. O. Brito, E. F. Marques, S. G. Silva, M. L. do Vale, P. Gomes, M. J. Araujo, J. E. Rodriguez-Borges, M. R. Infante, M. T. Garcia, I. Ribosa, M. P. Vinardell and M. Mitjans, *Colloids Surf., B*, 2009, **72**, 80; (*b*) M. R. Infante, L. Pérez, A. Pinazo, P. Clapés, M. C. Morán, M. Angelet, M. T. García and M. P. Vinardell, *C. R. Chim.*, 2004, **7**, 583; (*c*) L. Sánchez, M. Mitjans, M. R. Infante, M. T. García, M. A. Manresa and M. P. Vinardell, *Amino Acids*, 2007, **32**, 133.
5 N. Pérez, L. Pérez, M. R. Infante and M. T. García, *Green Chem.*, 2005, **7**, 540.
6 R. Vijay, S. Angayarkanny and G. Baskar, *Colloids Surf., A*, 2008, **317**, 643.
7 Y. Li, K. Holmberg and R. Bordes, *J. Colloid Interface Sci.*, 2013, **411**, 47.
8 (*a*) M. Gerova, F. Rodrigues, J. F. Lamère, A. Dobrev and S. Fery-Forgues, *J. Colloid Interface Sci.*, 2008, **319**, 526; (*b*) M. Takehara, *Colloids Surf.*, 1989, **38**, 149.
9 (*a*) R. O. Brito, E. F. Marques, P. Gomes, M. J. Araújo and R. Pons, *J. Phys. Chem. B*, 2008, **112**, 14877; (*b*) R. O. Brito, E. F. Marques, P. Gomes, S. Falcão and O. Söderman, *J. Phys. Chem. B*, 2006, **110**, 18158; (*c*) R. O. Brito, I. S. Oliveira, M. J. Araújo and E. F. Marques, *J. Phys. Chem. B*, 2013, **117**, 9400.
10 (*a*) L. Pérez, A. Pinazo, M. T. García, M. Lozano, A. Manresa, M. Angelet, M. P. Vinardell, M. Mitjans, R. Pons and M. R. Infante, *Eur. J. Med. Chem.*, 2009, **44**, 1884; (*b*) A. Mezei, L. Pérez, A. Pinazo, F. Comelles, M. R. Infante and R. Pons, *Langmuir*, 2012, **28**, 16761.
11 (*a*) A. Colomer, A. Pinazo, M. T. Garcia, M. Mitjans, M. P. Vinardell, M. R. Infante, V. Martinez and L. Pérez, *Langmuir*, 2012, **28**, 5900; (*b*) T. Mulsumoto, *J. Dispersion Sci. Technol.*, 1991, **12**, 503; (*c*) A. Colomer, A. Pinazo, M. A. Manresa, M. P. Vinardell, M. Mitjans, M. R. Infante and L. Pérez, *J. Med. Chem.*, 2011, **54**, 989.
12 (*a*) J. W. Frost, *WO Pat.*, 123669 A1, Michigan State University, 2005; (*b*) D. J. Fox, J. Reckless, S. M. Wilbert, I. Greig, S. Warren and D. J. Grainger, *J. Med. Chem.*, 2005, **48**, 867.
13 S. Y. Mhaskar, R. B. N. Prasad and G. Lakshminarayana, *J. Am. Oil Chem. Soc.*, 1990, **67**, 1016.
14 H. Ohshima, *Encyclopedia of Biocolloid and Biointerface Science*, John Wiley & Sons, Inc, 1st edn, 2016.
15 (*a*) L. Zhi, Q. Li, Y. Li and Y. Song, *Colloids Surf., A*, 2013, **436**, 684; (*b*) Y. Zhao, X. Yue, X. Wang, D. Huang and X. Chen, *Colloids Surf., A*, 2012, **412**, 90.
16 M. J. Rosen, *Surfactants and Interfacial Phenomena*, Wiley-Interscience, New York, 2nd edn, 1989.
17 B. Dong, X. Zhao, L. Zheng, J. Zhang, N. Li and T. Inoue, *Colloids Surf., A*, 2008, **317**, 666.
18 T. F. Svitova, Y. P. Smirnova, S. A. Pisarev and N. A. Berezina, *Colloids Surf., A*, 1995, **98**, 107.
19 T. Imae, Y. Takahashi and H. Muramatsu, *J. Am. Chem. Soc.*, 1992, **114**, 3414.
20 S. P. Moulik, M. E. Haque, P. K. Jana and A. R. Das, *J. Phys. Chem.*, 1996, **100**, 701.
21 K. Nyuta, T. Yoshimura, K. Tsuchiya, T. Ohkubo, H. Sakai, M. Abe and K. Esumi, *Langmuir*, 2006, **22**, 9187.
22 T. Patra, S. Ghosh and J. Dey, *J. Colloid Interface Sci.*, 2014, **436**, 138.
23 A. Ghosh and J. Dey, *Langmuir*, 2008, **24**, 6018.
24 (*a*) J. Sen and A. Chaudhuri, *Bioconjugate Chem.*, 2005, **16**, 903–912; (*b*) Y. I. González and E. W. Kaler, *Langmuir*, 2005, 7191; (*c*) D. R. Nogueira, M. Mitjans, M. C. Morán, L. Pérez and M. P. Vinardell, *Amino Acids*, 2012, **43**, 1203.
25 H. Zhang, L. Guo, Z. Xie, X. Xin, D. Sun and S. Yuan, *Langmuir*, 2016, **32**, 13736.
26 J. U. Kim, D. Schollmeyer, M. Brehmer and R. Zentel, *J. Colloid Interface Sci.*, 2011, **357**, 428.
27 G. Pabst, M. Rappolt, H. Amenitsch and P. Laggner, *Phys. Rev. E*, 2000, **62**, 4000.
28 A. Pinazo, L. Pérez, M. Lozano, M. Angelet, M. R. Infante, M. P. Vinardell and R. Pons, *J. Phys. Chem. B*, 2008, **112**, 8578.
29 L. Wang, X. Chen, Y. Chai, J. Hao, Z. Sui, W. Zhuang and Z. Sun, *Chem. Commun.*, 2004, 2840.